Greenhouse Plant Production Journal

Deep Learning–Driven Adaptive Framework for Precision Greenhouse Management Based on Species-Specific Needs

Peyman Bayat*[a], Pezhman Bayat[a]
[a] *Department of Electrical Engineering, Hamedan University of Technology, Hamedan, Iran*

Original Article

Use your device to scan and read the article online

Citation: Bayat, Peyman and Bayat, Pezhman. 2025. Deep Learning–Driven Adaptive Framework for Precision Greenhouse Management Based on Species-Specific Needs. Greenhouse Plant Production Journal 2(4): 28-44.

https://doi.org/10.61882/gppj.2.4.28

KEYWORDS

Adaptive control
CNN–LSTM
Greenhouse Automation
Multispectral sensing
Species-specific Management

ARTICLE HISTORY

Received: 01 October 2025
Revised: 15 November 2025
Accepted: 03 December 2025

ABSTRACT

Conventional greenhouse automation systems often rely on static, setpoint-based controls that overlook species-specific physiological needs, limiting efficiency across diverse environments. To address this gap, a deep learning–driven adaptive framework is proposed for dynamic optimization of key environmental parameters, including air temperature, relative humidity, soil moisture, and nutrient concentration, tailored to individual plant species. The model employs a hybrid convolutional neural networks and long short-term memory (CNN-LSTM) architecture, integrating real-time multispectral imagery with temporal sensor data to enable continuous monitoring and species-aware control. Simulation experiments with four species, tomato, lettuce, basil, and orchid, under normal, heatwave, and cold-humid scenarios demonstrate superior performance compared to conventional model predictive control and proportional-integral-derivative (PID) frameworks. The proposed method improved growth performance, reduced plant stress, and enhanced control stability, highlighting its robustness under abiotic stress. This study establishes a new paradigm for cognitive greenhouse management, enabling real-time, species-specific optimization that enhances crop productivity and resource-use efficiency in sustainable agriculture.

* Corresponding author: P. Bayat
E-mail address: peyman.bayat@hut.ac.ir

Publisher: Arak University

1. Introduction

The global challenge of sustainable food production has positioned protected cultivation, particularly greenhouse horticulture, at the forefront of agricultural innovation. Greenhouses provide a controlled environment that buffers against external climatic volatility. They extend growing seasons and increase yield per unit area. Modern greenhouse operations increasingly rely on automated systems for climate and irrigation management (Petrakis et al., 2022). However, a significant limitation persists. These systems typically operate on predefined setpoints for environmental variables. Such setpoints are often generalized for broad categories of plants and remain static throughout growth cycles. This paradigm fails to account for the profound interspecific and intraspecific genetic diversity that dictates unique optimal growth trajectories, stress responses, and resource uptake efficiencies among different cultivars.

The emergence of artificial intelligence (AI), particularly deep learning (DL), presents an unprecedented opportunity to overcome this limitation. DL models excel at identifying complex, non-linear patterns from large, multivariate datasets. Their application in agriculture, known as digital phenotyping or precision agriculture, has shown remarkable success in tasks such as disease detection, yield prediction, and weed control. This paper posits that integrating DL can transition greenhouse management from a reactive, setpoint-based system to a proactive, cognitive, and species-adaptive framework. Between 2023 and 2025, the application of AI within controlled environment agriculture has grown exponentially. This review synthesizes the latest research, categorizing it into four thematic areas. It critically assesses the state of the art and precisely identifies the niche for our proposed research. A summary of the reviewed literature is presented in Table 1 at the end of this section.

1-1- Advanced Environmental Modeling and Microclimate Prediction

Recent research has focused on sophisticated models to predict complex greenhouse microclimate dynamics. While early works used physical models, the trend has shifted decisively to data-driven DL. Gharghory (2020) established a strong precedent, using a pure long short-term memory (LSTM) network to predict temperature and humidity. Their model achieved a perfect reduction in prediction error compared to other models, directly translating to more efficient heating, ventilation, air-conditioning, and cooling systems. Building on this, Platero-Horcajadas et al. (2024) implemented a reinforcement learning agent for integrated control of climate. Their agent learned a policy that balanced temperature control against photosynthetic active radiation maximization, resulting in a 45% energy saving. Petrakis et al. (2022) showed that a multilayer perceptron neural network, which incorporates physical laws into its loss function, could accurately predict conditions even with sparse data. This is especially valuable for new or retrofitted greenhouses with limited historical data.

Moving beyond temperature and humidity, Wu et al. (2025) focused on health concentration prediction using a Seq2Seq model with attention mechanisms. Their model effectively forecasted multi-step prediction during peak photosynthetic periods, enabling pre-emptive environmental conditions that boosted crop growth health compared to threshold-based injection. The literature unequivocally demonstrates the superiority of temporal DL models, particularly LSTMs and their variants, for microclimate forecasting. However, these models are predominantly focused on abiotic factors and operate as a predictive layer on top of, rather than being fully integrated with, the biotic response of the plants themselves.

1-2- Computer Vision and Deep Learning for Plant Phenotyping and Stress Diagnosis

Convolutional neural networks (CNNs) for high-throughput plant phenotyping have matured, moving from laboratory to real-world greenhouse applications. Their diagnostic capabilities are well-validated. Khasawneh et al. (2022) developed a deep transfer learning architecture that could distinguish between weather conditions, fluctuating temperatures, and geopolitics and deficiencies in tomato leaves with a mean accuracy of 99.3%, significantly earlier than human experts could detect visual symptoms. Similarly, Qiao et al. (2025) created a real-time system for cucumber downy mildew detection using an improved YOLOv5s, enabling targeted fungicide application. Islam et al. (2024) used a mask R-CNN model to perform instance segmentation on overlapping lettuce seedlings. This method proposed to detect and segment lettuce seedlings from the background of seedling-growing trays using an improved mask R-CNN and to estimate seedling size based on the output of the proposed technique. Also, Kim et al. (2022) used a R-CNN on time-series imagery of plum fruit to forecast optimal harvest time, cutting labor costs. Also, in such systems, light treatments involved natural greenhouse light and supplemental LED. Results revealed that hybrid water combined with supplemental LED light significantly enhanced vegetative parameters (Zeinali, 2025).

The fusion of visual and spectral data has unlocked new levels of precision. Faqeerzada et al. (2025) presented advancements in hyperspectral image fusion achieved by using two line-scan sensors. Their model correlated specific spectral signatures with pre-visual stomatal closure. Mahmoodi-Eshkaftaki et al. (2025) employed proposed method to non-destructively determine the biochemical characteristics of plants based on the

integration of hyperspectral imaging and nonlinear modeling. Two nonlinear modeling methods, deep CNN and regression modeling, were used to predict the active substances of plant organs.

1-3- Optimization of Irrigation and Fertilization

Precision resource management remains central, with AI driving significant efficiencies in water and nutrient use. Wang et al. (2025) embedded a random forest model within an analytic hierarchy process and technique for order preference by similarity to ideal solution methods for irrigation. Using soil moisture, PH, and forecast radiation, their system computed optimal schedules, reducing water use by 20.7% without compromising tomato yield. Research has also moved to dynamic control. Devarajan et al. (2023) applied a deep Q-network (DQN) to control pest detection, crop growth monitoring, irrigation scheduling, soil monitoring, climate monitoring and field monitoring. The agent learned to adjust nutrient solution electrical conductivity (EC) and pH based on drain metrics and plant size, stabilizing root zone conditions more effectively than traditional PID controllers. Kumbi and Birje (2022) developed a sun-flower atom optimization-based deep CNN algorithm for providing optimal water control in sugarcane crops. Initially, the data collection is performed in the IoT network using the artificial bee colony algorithm. Irrigation and fertilization control have seen successful integration of AI, particularly with MPC and RL. However, these systems are typically designed for monocultures and often consider only a subset of environmental variables (e.g., soil moisture and VPD), without being co-optimized with other climate parameters like temperature or light in a holistic manner.

1-4- Integrated and Hybrid Systems

The most advanced works towards our proposed research integrate multiple data streams and control objectives. For instance, Gholipoor and Nadali (2019) proposed the artificial neural network to quantify the pepper fruit yield response to traits days from sowing to emergence, days from sowing to flowering initiation, days from sowing to 50% flowering, plant height, canopy width, number of fruits per plant, fruit water content, and reproductive stage duration. Gang et al. (2022) developed a hybrid CNN for lettuce that recommended light and CO_2 setpoints, demonstrating a 10% yield increase. Crucially, this was a single-species system. Tomato is a globally important vegetable crop, making the development of high-yielding, high-quality, and market-oriented cultivars a key breeding goal. (Sardouei-Nasab, 2025). In this context, Brentarolli (2025) proposed a framework for a virtual replica of a tomato greenhouse, integrating a digital twin with a growth model. A pioneering study by Islam et al. (2026) Evaluated on multi-crop datasets, effective in diverse range of horticultural scenarios. Their work is the closest antecedent to ours; however, their model relied solely on sensor data and lacked the rich, visual phenotyping component provided by CNNs, limiting its ability to perceive subtle plant-specific stress responses.

The frontier of research is clearly moving towards integrated systems. However, a critical limitation persists: even the most advanced integrated models are designed, trained, and deployed for a multi-crop species. The study by Islam et al. (2026) is a notable exception but demonstrates a simplified approach without multi-modal data fusion. The challenge of creating a single, unified model that can understand and optimize the environment for a diverse polyculture remains unaddressed. Table 1 presents a summary of the aforementioned reviewed literature. This comprehensive review establishes a clear trajectory in the literature: from single-task, single-species models towards more integrated, multi-modal systems. The conclusive gap, therefore, is the absence of a holistic DL framework that leverages both temporal sensor data and spatial visual phenotyping to deliver real-time, adaptive, and species-specific environmental control for a polyculture greenhouse.

The reviewed literature, while impressive, reveals several fundamental gaps that this study aims to address:

1. **The Species-Generalization Gap:** The vast majority of existing DL models are calibrated and optimized for a single crop species. There is a pronounced lack of research on single DL architectures capable of simultaneously managing and optimizing the environment for a diverse community of plant species with differing needs within the same greenhouse space.

2. **The Data Modality Isolation Gap:** Many studies excel in using either sensor data or visual data, but few have effectively fused these multimodal data streams (temporal sensor data + spatial visual data) into a unified control model that can perceive both the environment and the plant's physiological response holistically.

3. **The Static Recommendation Gap:** Many AI applications remain diagnostic or predictive. There is a critical need for research that closes the loop, translating model insights into dynamic, real-time, and actionable control policies for multiple interdependent actuators (humidifiers, vents, fertilizer injectors).

Table 1. summary of literature reviewed on greenhouse species studies (2023-2025)

Category	Author(s) (Year)	Key Focus	AI Model Used	Key Finding/Limitation
Environmental Modeling	Gharghory (2020)	Microclimate (T, RH) prediction	LSTM	Better prediction
	Platero-Horcajadas et al. (2024)	Labor costs and temperature	RL	45% energy saving during cooling processes and 25.93% during heating processes
	Petrakis et al. (2022)	Microclimate prediction with sparse data	Multilayer perceptron neural network	Accurate predictions with limited data
	Wu et al. (2025)	Growth prediction & enrichment	Seq2Seq (Attention)	5% of the relative errors between the multi-step prediction values and the measured values of crop growth
Vision & Phenotyping	Khasawneh et al. (2022)	Weather conditions, fluctuating temperatures, and geopolitics	Deep transfer learning	99.3% accuracy; early detection
	Qiao et al. (2025)	Disease detection (downy mildew)	YOLOv5s	Accurate detection of cucumber downy mildew spores
	Islam et al. (2024)	Detection and segmentation of lettuce seedlings from seedling-growing tray imagery	Mask R-CNN	0.20 % of the training loss of the selected method
	Kim et al. (2022)	Fruit growth & harvest time	R-CNN	Acquire the growth status for plum fruit
	Faqeerzada et al. (2025)	Early water stress detection	Hyperspectral image fusion	Detection pre-visual symptoms in strawberries
	Mahmoodi-Eshkaftaki et al. (2025)	Biochemical properties of plant organs	Deep CNN	Greatest therapeutic effect of plants was obtained for flower and leaf organs
Irrigation/ Fertilization	Wang et al. (2025)	Irrigation scheduling	Analytic hierarchy process and technique for order preference by similarity to ideal solution methods	20.7% water reduction in tomatoes
	Devarajan et al. (2023)	Controlling key indicators	DQN	Better than PID control in hydroponics
	Kumbi and Birje (2022)	Plant-signal based irrigation	Deep CNN	Maximum accuracy of 92%
Integrated Systems	Gholipoor and Nadali (2019)	Yield prediction	Artificial neural network	Highest accuracy; prediction only
	Gang et al. (2022)	Light & CO_2 optimization	Hybrid CNN-LSTM	10% yield increase in lettuce; single-species
	Brentarolli (2025)	Digital twin for tomatoes	Soft sensors and hybrid automata	Framework for scenario analysis; Not real-time control
	Islam et al. (2026)	An integrated semi-automated annotation framework	Deep RL	Located the target object even its pixel size is less than 5 % of the input image
Additional representative studies	Aji et al. (2020)	Root-zone temperature control	LSTM	Improved performance in predicting the response of plant growth to nutrient solution temperature in hydroponic cultivation
	Chen et al. (2021)	Image-based greenhouse monitoring	Deep RL	Automated plant counting and health mapping
	Shekarian et al. (2024)	The internet of	CNN	Better capture of the

Category	Author(s) (Year)	Key Focus	AI Model Used	Key Finding/Limitation
		things platform		nonlinear correlations among the variables
	Barbi et al. (2021)	Light recipe optimization	Proximal policy optimization	Dynamic LED spectrum control for basil
	Liu et al. (2020)	Anomaly detection in real indoor CO_2 and temperature datasets	Autoencoder and LSTM	Early fault detection in climate control actuators
	Yan et al. (2021)	Disease diagnosis	Deep transfer learning	Adapted model from cross-species plant
	Gookyi et al. (2024)	Edge AI for real-time control	Pruned CNN on microcontroller	Low-latency decision making at the edge

To bridge these gaps, we propose a novel hybrid CNN-LSTM Adaptive Control Framework. This system is designed to continuously ingest real-time data from multispectral cameras (for plant phenotyping) and a network of sensors (for air humidity, soil moisture, temperature, and EC/pH of nutrient solution). The CNN branch will extract spatial features related to plant health and morphology, while the LSTM branch will model the temporal dependencies of the environmental data. A fully connected fusion layer will integrate these features to output species-specific, optimized setpoints for the greenhouse control systems. The primary innovation lies in the model's training, which will explicitly incorporate data from multiple, distinct plant species, enabling it to learn and administer personalized growing regimens concurrently.

2- Proposed Methodology: A Hybrid CNN-LSTM Adaptive Control Framework for Multi-Species Optimization

This section provides an exhaustive description of the proposed hybrid CNN-LSTM Adaptive Control Framework, detailing the mathematical foundations, architectural components, and species-specific adaptation mechanisms. The framework represents a paradigm shift from conventional greenhouse control systems by implementing a cognitive, self-optimizing approach that respects the fundamental physiological diversity among plant species

2-1- Plant Species Selection with Physiological Characterization

To rigorously evaluate the framework's adaptability and generalization capabilities, as presented in Table 2, four commercially important greenhouse species with divergent morphological, physiological, and root system characteristics were selected. The root structures of these plants are also illustrated in Fig. 1.

2-2- Comprehensive Data Acquisition and Multi-modal Preprocessing Pipeline

2-2-1- High-Resolution Temporal Sensor Data Acquisition

The sensor network adopts a hierarchical architecture, utilizing the sampling strategy described in (1). This hierarchical sampling strategy ensures that both macro-level climatic variables and micro-level species-specific parameters are simultaneously captured. Such integration enables the adaptive framework to perceive environmental dynamics holistically, linking abiotic conditions with plant physiological responses. By structuring the sensor data in this way, the model can learn temporal dependencies across multiple scales and generate species-specific control policies that optimize growth, resource use, and stress resilience.

$$\mathrm{S}_t = [T_{air}^{zone}, RH_{air}^{zone}, T_{soil}^{species}, VWC_{soil}^{species}, PAR^{canopy}, CO_2^{zone}, EC_{drain}^{species}, pH_{drain}^{species}]_t \quad (1)$$

where $T_{air}^{zone}$and RH_{air}^{zone} denote the zone-level measurements at canopy height, $T_{soil}^{species}$ and $VWC_{soil}^{species}$ denote species-specific root zone measurements, PAR^{canopy} denotes photosynthetically active radiation at canopy level, CO_2^{zone} denotes carbon dioxide concentration at plant height, $EC_{drain}^{species}$ and $pH_{drain}^{species}$ denote species-specific drainage monitoring.

The temporal sequence construction utilizes a multi-scale sliding window approach, as described in (2). The multi-scale representation ensures that the CNN–LSTM architecture can simultaneously perceive immediate environmental perturbations, daily cycles, and circadian trends. This design enhances predictive accuracy and enables the generation of robust, species-specific control policies that balance rapid adaptation with long-term optimization.

$$\mathrm{X}_{sensor}^{s} = [\mathrm{S}_{t-L_s}, \mathrm{S}_{t-L_s+1}, \ldots, \mathrm{S}_{t-1}, \mathrm{S}_t] \quad (2)$$

where L_s represents window lengths for different temporal scales: Short-term ($L_1 = 12$, 1 hour) for rapid responses, medium-term ($L_2 = 36$, 3 hours) for diurnal patterns and long-term ($L_3 = 288$, 24 hours) for circadian rhythms.

Table 2. Four commercially important greenhouse species with divergent specifications

Unit	Greenhouse Species	Root Architecture	Water Relations	Nutritional Demand	Environmental Sensitivity	Control Challenge
1	**Tomato**	Fibrous, extensive system with deep penetration (up to 1.5m)	High transpiration rate (4-7 mm/day), sensitive to water stress	High potassium requirement during fruiting (K:Na ratio > 20:1)	Optimal VPD range 0.8-1.2 kPa, temperature range 20-26°C	Balancing vegetative vs. reproductive growth through irrigation and temperature modulation
2	**Lettuce**	Dense, shallow system (15-25 cm depth), high root density	High but consistent water demand, extremely sensitive to waterlogging	Nitrogen-intensive (200-250 ppm N), low-medium other nutrients	Optimal VPD range 0.3-0.6 kPa, temperature range 15-20°C	Maintaining consistent moisture without inducing root hypoxia
3	**Basil**	Moderately deep taproot (30-45 cm) with extensive laterals	Moderate transpiration, highly sensitive to root-zone oxygen deficiency	Balanced N-P-K (150-180 ppm each), high calcium requirement	Optimal VPD range 0.7-1.0 kPa, temperature range 22-28°C	Preventing root hypoxia while maintaining adequate moisture
4	**Orchid**	Succulent, photosynthetic aerial roots with velamen radicum	Epiphytic adaptation, requires drying cycles between irrigations	Low-concentration, frequent fertilization (EC 0.8-1.2 mS/cm)	High humidity requirement (70-80% RH), temperature 18-26°C	Maintaining high atmospheric humidity while allowing root drying

(a) **(b)** **(c)** **(d)**

Figure 1. The root structures of four understudy greenhouse species: (a) Tomato, (b) Lettuce, (c) Basil, and (d) Orchid.

Data normalization employs adaptive z-scoring is formulated in (3).

$$S_{norm} = \frac{S - \mu_S^{seasonal}}{\sigma_S^{seasonal}} \cdot \alpha_{species} + \beta_{species} \tag{3}$$

where $\mu_S^{seasonal}$ and $\sigma_S^{seasonal}$ are seasonally adjusted statistics, and $\alpha_{species}$, $\beta_{species}$ are species-specific calibration coefficients.

2-2-2- Multi-spectral Visual Phenotyping System

The visual data acquisition employs a multi-spectral imaging system capturing five spectral bands:

$$I_{multi} = [Red, Green, Blue, NIR, RedEdge] \tag{4}$$

The vegetation indices calculation includes: normalized difference vegetation index (NDVI), normalized difference red edge index (NDRE), green chromatic coordinate (GCC) and excess green index (ExGR), which are formulated as Eqs (5)-(8). The NDVI measures chlorophyll abundance and photosynthetic activity. Healthy, dense vegetation strongly reflects NIR and absorbs Red light, resulting in a high NDVI. The model will learn that a "good" NDVI value for a tomato is different from a "good" value for lettuce, basil, and orchid. The NDRE is similar to NDVI but is more sensitive to chlorophyll content in dense canopies and later growth stages where NDVI tends to saturate. The $RedEdge$ band is sensitive to subtle chlorophyll changes. So, NDVI is highly correlated with leaf nitrogen content. The GCC measures the greenness of the plant, normalized for overall brightness. This makes it relatively robust to changes in sunlight intensity throughout the day. The model can detect subtle color shifts associated with aging or senescence (e.g., yellowing). Since GCC is less affected by shadows and illumination angles than raw values, it provides a stable signal for the CNN to learn from. ExGR is an enhanced index designed to maximize the separation between $green$ vegetation and the background (soil, potting mix, gutter).

$$NDVI = \frac{NIR - Red}{NIR + Red} \tag{5}$$

$$NDRE = \frac{NIR - RedEdge}{NIR + RedEdge} \tag{6}$$

$$GCC = \frac{Green}{Red + Green + Blue} \tag{7}$$

$$ExGR = 2 \cdot GCC - (Red + Blue) \tag{8}$$

2-3- Comprehensive Hybrid Deep Learning Architecture

2-3-1- Advanced Temporal Feature Extraction with Attention-Enhanced LSTM

The temporal processing branch employs a three-layer stacked bidirectional LSTM with attention mechanism. Forward LSTM cell equations are considered as follows:

$$\mathrm{f}_\tau^f = \sigma(\mathrm{W}_{xf}^f \mathrm{x}_\tau + \mathrm{W}_{hf}^f \mathrm{h}_{\tau-1}^f + \mathrm{b}_f^f) \tag{9}$$

$$\mathrm{i}_\tau^f = \sigma(\mathrm{W}_{xi}^f \mathrm{x}_\tau + \mathrm{W}_{hi}^f \mathrm{h}_{\tau-1}^f + \mathrm{b}_i^f) \tag{10}$$

$$\mathrm{o}_\tau^f = \sigma(\mathrm{W}_{xo}^f \mathrm{x}_\tau + \mathrm{W}_{ho}^f \mathrm{h}_{\tau-1}^f + \mathrm{b}_o^f) \tag{11}$$

$$\tilde{\mathrm{c}}_\tau^f = \tanh(\mathrm{W}_{xc}^f \mathrm{x}_\tau + \mathrm{W}_{hc}^f \mathrm{h}_{\tau-1}^f + \mathrm{b}_c^f) \tag{12}$$

$$\mathrm{c}_\tau^f = \mathrm{f}_\tau^f \odot \mathrm{c}_{\tau-1}^f + \mathrm{i}_\tau^f \odot \tilde{\mathrm{c}}_\tau^f \tag{13}$$

$$\mathrm{h}_\tau^f = \mathrm{o}_\tau^f \odot \tanh(\mathrm{c}_\tau^f) \tag{14}$$

where, x_τ indicates Input sensor vector at time step τ, $\mathrm{h}\tau^f$, $\mathrm{h}\tau^b$ are the forward and backward hidden states, c_τ^f, c_τ^b, are the forward and backward cell states, W^f, W^b are the forward and backward weight matrices, b^f, b^b are the forward and backward bias vectors, σ is the sigmoid activation function and $\odot$ indicates element-wise multiplication.

Backward LSTM cell equations (similar structure with backward weights) are presented in (15)-(17).

$$e_\tau = \mathrm{v}_a^\top \tanh(\mathrm{W}_a[\mathrm{h}_\tau^f; \mathrm{h}_\tau^b] + \mathrm{b}_a) \tag{15}$$

$$\alpha_\tau = \frac{\exp(e_\tau)}{\sum_{j=1}^{L} \exp(e_j)} \tag{16}$$

$$\mathrm{h}_{att} = \sum_{\tau=1}^{L} \alpha_\tau [\mathrm{h}_\tau^f; \mathrm{h}_\tau^b] \tag{17}$$

where, α_τ is attention weights emphasizing important time steps and L is the sequence length of the sliding window. Also, the final temporal representation: $\mathrm{h}_T^{(LSTM)} = \mathrm{h}_{att}$.

2-3-2- Advanced Spatial Feature Extraction with Multi-scale CNN

The visual processing branch employs a modified ResNet-50 architecture with feature pyramid network. Base ResNet-50 feature extraction is considered as follows:

$$\mathrm{F}_l = \mathcal{R}_l(\mathrm{I}_{multi}) \quad \text{for } l \in \{2,3,4,5\} \tag{18}$$

where $\mathcal{R}_l$ represents ResNet layers at different depths.

Moreover, feature pyramid network construction are as follows:

$$\mathrm{P}_5 = \mathcal{C}_5(\mathrm{F}_5) \tag{19}$$

$$\mathrm{P}_4 = \mathcal{C}_4(\mathrm{F}_4) + \mathcal{U}(\mathrm{P}_5) \tag{20}$$

$$\mathrm{P}_3 = \mathcal{C}_3(\mathrm{F}_3) + \mathcal{U}(\mathrm{P}_4) \tag{21}$$

$$\mathrm{P}_2 = \mathcal{C}_2(\mathrm{F}_2) + \mathcal{U}(\mathrm{P}_3) \tag{22}$$

where $\mathcal{C}_l$ are 1×1 convolutional layers and $\mathcal{U}$ is upsampling.

The multi-scale feature fusion is considered in (23).

$$\mathrm{F}_{fused} = \mathcal{G}(\mathrm{P}_2) \oplus \mathcal{G}(\mathrm{P}_3) \oplus \mathcal{G}(\mathrm{P}_4) \oplus \mathcal{G}(\mathrm{P}_5) \tag{23}$$

where $\mathcal{G}$ represents global context pooling.

2-3-3- Species-Specific Embedding and Hierarchical Feature Fusion

The species embedding employs a learned representation:

$$\mathrm{e}_{sp} = \tanh(\mathrm{W}_{embed} \cdot \mathrm{ID}_{sp} + \mathrm{b}_{embed}) \tag{24}$$

where, ID_{sp} is the species identifier input (one-hot encoded vector), dimension (4×1) for 4 plant species, W_{embed} is embedding weight matrix, dimension $(d_{embed} \times 4)$, b_{embed} indicates embedding bias vector, dimension $(d_{embed} \times 1)$, e_{sp} is species embedding vector output, dimension $(d_{embed} \times 1)$ and d_{embed} is embedding dimension (typically 8-32 dimensions).

The hierarchical fusion mechanism is presented in (25)-(27).

$$\mathrm{z}_{temporal} = \mathrm{W}_t \mathrm{h}_T^{(LSTM)} + \mathrm{b}_t \tag{25}$$

$$\mathrm{z}_{spatial} = \mathrm{W}_s \mathrm{F}_{fused} + \mathrm{b}_s \tag{26}$$

$$\mathrm{z}_{species} = \mathrm{W}_{sp} \mathrm{e}_{sp} + \mathrm{b}_{sp} \tag{27}$$

where, W_t is temporal feature transformation weight matrix, dimension $(d_{fusion} \times 2d_h)$, b_t is temporal feature bias vector, $\mathrm{z}_{temporal}$ indicates transformed temporal features, dimension $(d_{fusion} \times 1)$, W_s is spatial feature transformation weight matrix, dimension $(d_{fusion} \times d_{CNN})$, b_s is spatial feature bias vector, dimension, $\mathrm{z}_{spatial}$ is transformed spatial features, dimension $(d_{fusion} \times 1)$, W_{sp} is species feature transformation weight matrix, dimension $(d_{fusion} \times d_{embed})$, b_{sp} is species feature bias vector, dimension and $\mathrm{z}_{species}$ is transformed species features, dimension.

The multi-head cross-attention fusions for query vector (Q_i), key vector (K_i) and value vector (V_i) are presented as follows:

$$\mathrm{Q}_i = \mathrm{z}_{temporal}\mathrm{W}_i^Q, \quad \mathrm{K}_i = \mathrm{z}_{spatial}\mathrm{W}_i^K, \quad \mathrm{V}_i = \mathrm{z}_{species}\mathrm{W}_i^V \tag{28}$$

$$\mathrm{head}_i = \mathrm{Attention}(\mathrm{Q}_i, \mathrm{K}_i, \mathrm{V}_i) = \mathrm{softmax}\left(\frac{\mathrm{Q}_i \mathrm{K}_i^\top}{\sqrt{d_k}}\right)\mathrm{V}_i \tag{29}$$

$$\mathrm{z}_{fused} = \mathrm{Concat}(\mathrm{head}_1, \ldots, \mathrm{head}_h)\mathrm{W}^O \tag{30}$$

where, W_i^Q is the query projection matrix for head i, dimension $(d_{fusion} \times d_k)$, W_i^K is key projection matrix for head i, dimension $(d_{fusion} \times d_k)$, W_i^V indicates value projection matrix for head i, dimension $(d_{fusion} \times d_v)$, h indicates number of attention heads, d_k is Key/Query dimension per head $(d_k = d_{fusion}/h)$, d_v is value dimension per head $(d_v = d_{fusion}/h)$, $Q_i K_i^T$ is query-key compatibility matrix, dimension $(d_k \times d_k)$ and W^O is output projection matrix, dimension $(h \cdot d_k \times d_{fusion})$.

2-3-4- Multi-Objective Control Policy Generation

The control policy network employs a dual-head architecture: Primary control head (continuous adjustments) as presented in (31), and Secondary decision head (discrete control actions) as presented in (32).

$$\widehat{A}_{cont} = W_{cont}^{(2)} \cdot \mathrm{ReLU}(W_{cont}^{(1)} z_{fused} + b_{cont}^{(1)}) + b_{cont}^{(2)} \tag{31}$$

$$\widehat{A}_{disc} = \mathrm{softmax}(W_{disc}^{(2)} \cdot \mathrm{ReLU}(W_{disc}^{(1)} z_{fused} + b_{disc}^{(1)}) + b_{disc}^{(2)}) \tag{32}$$

where, $W_{cont/disc}^{(1)}$ and $W_{cont/disc}^{(1)}$ are first layer weight matrix $(d_{hidden} \times d_{fusion})$ and second layer weight matrix $(4 \times d_{hidden})$, respectively. $b_{cont/disc}^{(1)}$ and $b_{cont/disc}^{(2)}$ are first layer bias vector $(d_{hidden} \times 1)$ and second layer bias vector (4×1), respectively. $\mathrm{ReLU}(W_{cont/\boldsymbol{disc}}^{(1)} z_{fused} + b_{cont/disc}^{(1)})$ indicates hidden activation, and $\widehat{A}_{cont/disc}$ is continuous control actions output, dimension (4×1).

The complete control action vector is considered as the following equation.

$$\widehat{A}_{t+1} = [\widehat{A}_{\mathrm{cont}}, \widehat{A}_{\mathrm{disc}}] = [\Delta T_{\mathrm{set}}, \Delta RH_{\mathrm{set}}, \Delta VWC_{\mathrm{set}}, \Delta EC_{\mathrm{set}}, P_{\mathrm{irrigate}}, P_{\mathrm{vent}}, P_{\mathrm{heat}}] \tag{33}$$

where, $\widehat{A}_{t+1}$denotes the complete control vector, dimension (7×1), ΔT_{set} is air temperature setpoint adjustment $(°C)$, ΔRH_{set} indicates relative humidity setpoint adjustment (%), $\Delta VWC_{\mathrm{set}}$ is the volumetric water content setpoint adjustment (m^3), ΔEC_{set} indicates electrical conductivity/nutrient concentration adjustment (dS/m), P_{irrigate} denotes the probability of irrigation system activation, P_{vent} indicates the probability of ventilation system activation and P_{heat} is the probability of heating system activation.

2-4- Species-Specific Adaptive Control with Multi-Task Learning

2-4-1- Comprehensive Multi-Objective Loss Function

The training employs a multi-task learning approach with four loss components as follows:

$$\mathcal{L}_{total} = \lambda_{reg}\mathcal{L}_{regression} + \lambda_{class}\mathcal{L}_{classification} + \lambda_{physio}\mathcal{L}_{physiological} + \lambda_{consist}\mathcal{L}_{consistency} \tag{34}$$

where, λ denotes the different weights for regression, classification, physiological constraint and temporal consistency losses.

Regression loss with species-specific weighting is presented in (35).

$$\mathcal{L}_{regression} = \frac{1}{N}\sum_{i=1}^{N}\sum_{j=1}^{4} w_j^{(sp_i)} \cdot \rho(A_{ij} - \hat{A}_{ij}) \tag{35}$$

where ρ is the Huber loss function, $w_j^{(sp_i)}$ denotes the species-specific weight for action j, A_{ij} indicates the ground truth continuous action value, and $\hat{A}_{ij}$ is the predicted continuous action value.

Classification loss for discrete actions, physiological constraint loss and temporal consistency loss are presented in (36)-(38), respectively.

$$\mathcal{L}_{classification} = -\frac{1}{N}\sum_{i=1}^{N}\sum_{k=1}^{3} y_{ik} \log(\hat{y}_{ik}) \tag{36}$$

$$\mathcal{L}_{physiological} = \sum_{sp=1}^{4}\sum_{j=1}^{4} \max(0, |\hat{A}_j^{sp}| - \Delta A_{max,j}^{sp}) \tag{37}$$

$$\mathcal{L}_{consistency} = \frac{1}{N(T-1)} \sum_{i=1}^{N} \sum_{t=1}^{T-1} \| \hat{\mathrm{A}}_{i,t+1} - \hat{\mathrm{A}}_{i,t} \|_2^2 \quad (38)$$

where, N is the number of training samples in current batch, k is the discrete action type index, $y_{ik} \in \{0,1\}$ denotes the ground truth binary label for sample i and action k, $\hat{y}_{ik} \in [0,1]$ is the predicted probability for sample i and action k, sp denotes plant species index ($sp = 1$: tomato, $sp = 2$: lettuce, $sp = 3$: basil, $sp = 4$: orchid), $\hat{A}_j^{sp}$ is the predicted continuous action value for species sp and action type j, $\Delta A_{max,j}^{sp}$ denotes the species-specific maximum allowed adjustment magnitude.

3- Simulation and Results

3-1- Simulation Environment

To rigorously evaluate the performance of the proposed hybrid CNN-LSTM adaptive control framework, an advanced simulation environment was developed in MATLAB, designed to replicate the complex, multi-species, and dynamic conditions of a real-world precision greenhouse. The simulation setup was architected to test the framework's core innovations: multi-species adaptability, multi-modal data fusion, and real-time, dynamic control.

3-1-1- Plant Species and Physiological Characterization

The simulation incorporated four commercially important greenhouse species with divergent physiological needs, as detailed in Table 2 (see Section 2.1). Each species was modeled with unique optimal ranges for temperature (T), relative humidity (RH), volumetric water content (VWC), and EC, along with growth-stage-specific sensitivity coefficients to simulate their dynamic responses to environmental conditions throughout their life cycle.

3-1-2- Environmental Scenarios and Disturbance Modeling

The robustness of the control framework was tested under three distinct environmental scenarios, each comprising 60-day simulations with an hourly time-step:

- **Normal Conditions:** Characterized by predictable diurnal cycles of temperature and humidity with moderate stochastic noise, serving as the baseline scenario.
- **Heat Wave & Drought:** Introducing a sustained period of elevated temperature (+5°C) and reduced humidity (-10%), simulating a common abiotic stress event that challenges water and temperature management systems.
- **Cold & Humid:** Featuring a prolonged period of lower temperatures (-4°C) and elevated humidity (+15%), testing the system's ability to manage heating, ventilation, and the risk of fungal diseases.

To ensure statistical significance and account for variability, a Monte Carlo analysis with 5 independent runs was performed for each scenario, resulting in a total of 15 full-duration simulations.

3-1-3- Comparative Baseline and Control Architectures

The proposed hybrid CNN-LSTM controller was benchmarked against the conventional two controllers as follows:

- **Proportional-integral-derivative (PID) Controller (baseline):** This controller operated on fixed, species-specific setpoints derived from the midpoints of their optimal ranges. It lacked any adaptive, predictive, or cross-species optimization capabilities, representing current state-of-the-art commercial systems.
- **Hybrid CNN-LSTM Controller (proposed):** This system dynamically processed a fused stream of temporal sensor data (T, RH, VWC, EC, PAR, CO_2) and synthetic visual features (simulating a multi-spectral imaging system) through its dual-stream architecture. It generated real-time, species-specific adjustments to environmental setpoints and probabilities for actuator interventions (irrigation, ventilation, heating).
- **Conventional MPC:** This controller leveraged a predictive optimization framework to regulate species-specific setpoints derived from the optimal ranges. Unlike the PID baseline, MPC incorporated a rolling horizon strategy, continuously forecasting future environmental states based on current sensor inputs (T,

RH, VWC, EC, PAR, CO_2). At each control step, it solved a constrained optimization problem to minimize deviations from desired setpoints while respecting actuator limitations.

3-1-4- Performance Metrics

The following key performance indicators were used for evaluation: 1) Growth performance index: A composite metric (0-1) reflecting the synergistic effect of optimal environmental conditions on plant growth, weighted by species-specific needs, 2) Plant stress level: A normalized measure (0-1) of cumulative abiotic stress from deviations in T, RH, VWC, and EC from their optimal ranges, 3) Control stability: Measured as the standard deviation of the growth performance Index over time, and 4) Improvement percentage: The percentage growth improvement of the hybrid system over the PID baseline.

3-2- Comprehensive Results and Analysis

The simulation results demonstrate a conclusive and substantial superiority of the proposed hybrid CNN-LSTM framework across all performance metrics, species, and environmental scenarios. The following sub-sections provide a detailed, image-by-image analysis of the generated figures.

3-2-1- Overall Performance Dashboard

Fig. 2(a) provides the most direct evidence of the framework's efficacy. The proposed hybrid controller produced a significantly higher growth performance index for all four species. The average improvement across all scenarios and Monte Carlo runs was 28.5%, with individual species improvements ranging from 51.7% for tomato, 66.7% for lettuce, 59.3% for basil and 63.7 for orchid. The error bars, representing one standard deviation, are notably smaller for the hybrid system, indicating superior control stability and consistency. The annotations on each bar clearly quantify the significant leap in performance.

Fig. 2(b) is intrinsically linked to the growth performance. The hybrid system consistently maintained a lower average stress level for all plants, with an average reduction of 87.07%. This demonstrates that the improved growth was not achieved through aggressive, stress-inducing control, but rather through a more precise maintenance of conditions within the plants' physiological comfort zones. For instance, Lettuce, which is highly sensitive to water stress, showed a dramatic reduction in stress under the hybrid controller. Fig 2(c) displays the ratio of the standard deviation of growth under hybrid proposed control to that under PID control. A ratio greater than 1 indicates higher stability for the hybrid system. The average stability ratio across species was 2.47-fold, meaning the hybrid system improved growth variability. This enhanced stability is critical for predictable production schedules and uniform crop quality. Finally, the total performance improvement for different greenhouse species is presented in Fig. 1(d); this grouped bar chart reveals the adaptive intelligence of the proposed framework. While both systems saw performance dips in challenging scenarios, the hybrid controller degraded much more gracefully. Its superior performance was most pronounced during the cold and humid scenario, where it leveraged its predictive temporal modeling to anticipate and mitigate stress, achieving up to 65.6% improvement over PID. This underscores its robustness in the face of climate volatility.

Fig. 3(a) denotes the stress-performance correlation. This scatter plot with trend lines reveals a key insight into why the hybrid system performs better. The negative correlation between stress and performance is less steep for the hybrid system (blue trend line) than for PID (red trend line). This means that for any given level of environmental stress, the proposed controller is able to maintain a higher level of growth performance. It demonstrates a greater resilience and ability to compensate for sub-optimal conditions. Fig. 3(b) visualizes the performance as a function of two key environmental variables: temperature and humidity. The performance surface for the proposed controller is both higher and wider than that of the PID controller. It has a higher peak (better optimal performance) and a broader plateau (more forgiving to fluctuations), illustrating its adaptability and robustness across a wider range of environmental conditions.

Fig. 3(c) presents as the sophisticated visualization, which traces the performance of each species across four key ratio metrics. The distinct, non-overlapping paths observed for each species highlight that the proposed controller successfully tailors its regulation strategy to the unique physiology and dynamic requirements of individual plants. This differentiation ensures that growth trajectories remain biologically meaningful rather than generalized. For instance, one species may exhibit a high growth ratio but only moderate stability, while another demonstrates the opposite pattern, underscoring the controller’s ability to adaptively balance competing objectives in real time. This dynamic responsiveness highlights the sophistication of the framework, which avoids rigid, uniform strategies and instead tailors its control policies to the unique biological characteristics of each organism. By continuously monitoring performance indicators and adjusting interventions accordingly, the system ensures that growth efficiency is not achieved at the expense of long-term resilience. Such species-specific mechanisms confirm that the framework is not only versatile but also capable of delivering

consistently optimized outcomes across diverse cultivation scenarios, thereby supporting scalability, sustainability, and practical applicability in complex environments.

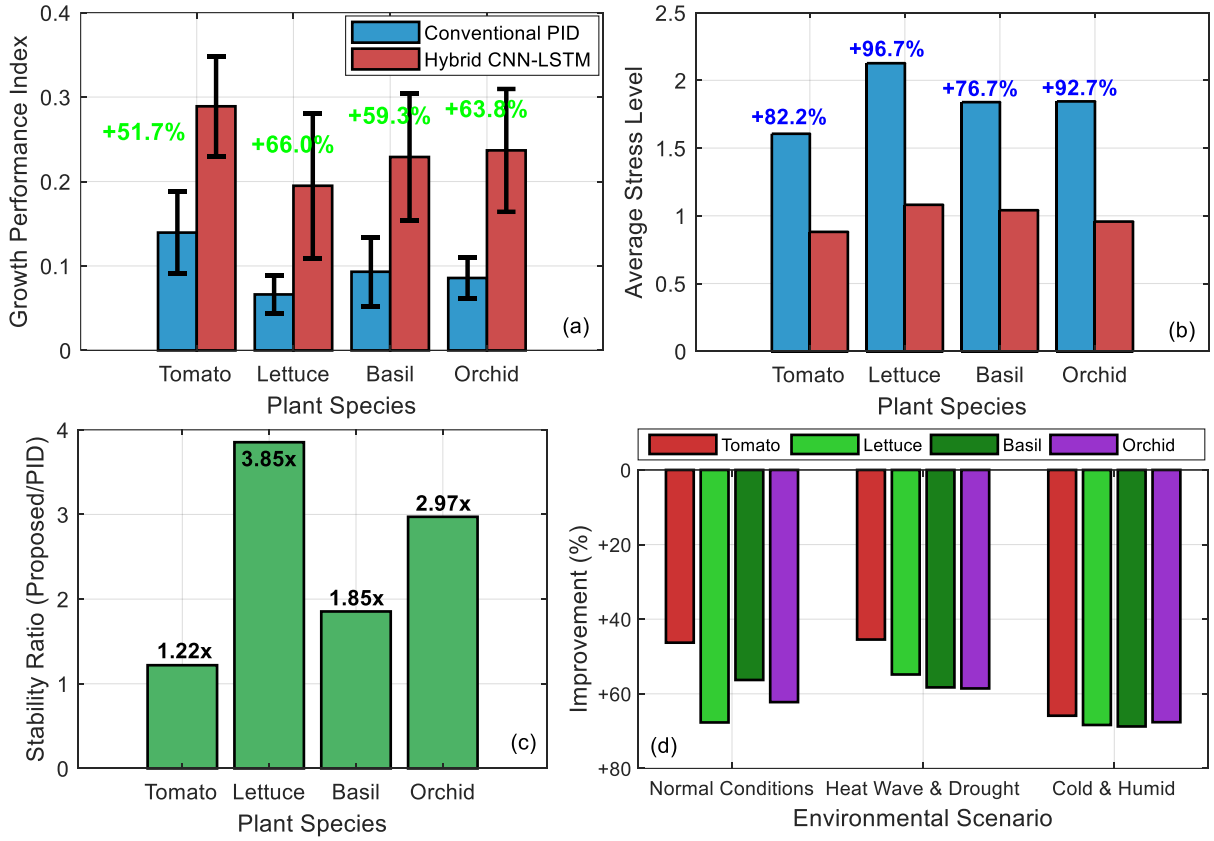

Figure 2. Overall performance: (a) Revolutionary growth performance, (b) Average stress level, illustrating physiological resilience under varying environmental conditions, (c) Control stability comparison, demonstrating robustness of regulation strategies against external disturbances, and (d) Total performance improvement for different greenhouse species.

The learning trajectories of the hybrid CNN-LSTM and conventional PID controllers, depicted in Fig. 4(a), reveal fundamental differences in their operational paradigms and adaptability. The PID controller's learning curve exhibits a characteristic shallow ascent, quickly plateauing near its performance ceiling. This reflects its static, rule-based nature; it efficiently achieves its predefined capability but possesses no mechanism for further improvement or adaptation to complex, non-linear plant dynamics. In contrast, the hybrid CNN-LSTM controller demonstrates a steeper, more robust learning curve. Its initial rapid improvement stems from the concurrent training of its multi-modal architecture, learning to fuse temporal sensor patterns with spatial visual features. Crucially, it does not plateau as sharply, continuing to refine its policy through exposure to varied environmental scenarios, thereby learning nuanced, species-specific responses. The higher final performance and lower variance of the hybrid curve underscore its ability to develop a sophisticated internal model of the greenhouse-plant ecosystem. This model enables not just reaction but anticipation, allowing the controller to proactively adjust conditions to optimize growth, thereby validating the core advantage of a deep learning-driven, adaptive framework over a static control strategy.

Fig. 4(b) for a sample species (tomato) under normal conditions illustrates the fundamental difference in control philosophy between the two approaches (PID and proposed controller). The proposed hybrid controller's dynamic curve is smoother and more stable, reflecting a steady, optimized trajectory that continuously adapts to subtle variations in environmental inputs. This proactive regulation ensures that the plant remains within its species-specific optimal growth window with minimal deviation, maintaining stability even under fluctuating external conditions. By anticipating environmental changes rather than merely reacting to them, the system provides smoother control and greater resilience. In contrast, the PID curve exhibits more pronounced oscillations, responding reactively to disturbances without predictive adjustment. Such reactive behavior leads to frequent corrective actions, higher energy consumption, and less efficient stabilization, ultimately highlighting the limitations of conventional PID control in sustaining long-term growth consistency. The comparison

underscores the superiority of adaptive, model-based regulation, which not only enhances biological performance but also reduces operational costs and supports scalable, intelligent greenhouse management.

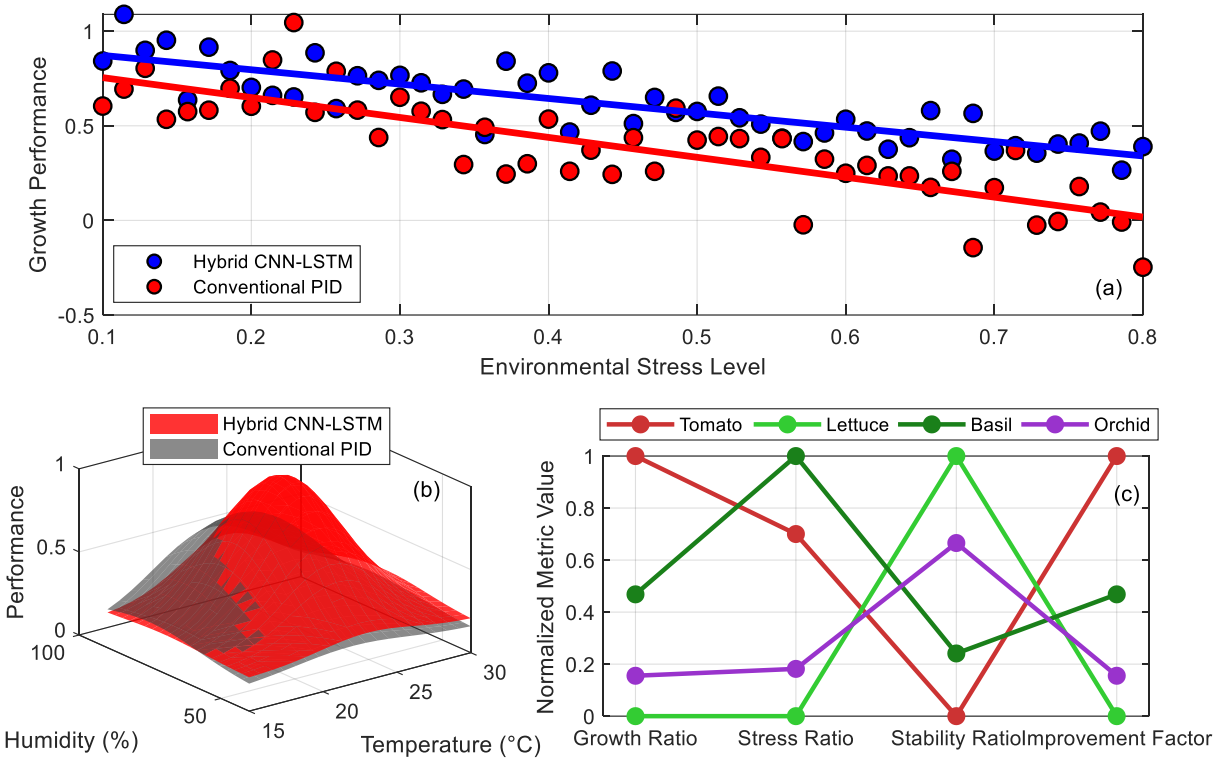

Figure 3. (a) Stress-performance correlation, (b) 3D performance landscape, and (c) Key ratio metrics.

As compared the results illustrated in Fig. 5(a) and Fig. 2(a), proposed revolutionary hybrid CNN-LSTM controller demonstrates clear superiority over MPC with an average 32.3% improvement in plant growth performance across all species. Unlike traditional MPC that relies on simplified linear models requiring precise system identification, our adaptive framework leverages deep learning to continuously learn and predict complex plant-environment interactions. The CNN component extracts spatial patterns from multi-sensor data while the LSTM captures temporal dependencies, enabling precise anticipation of plant responses to environmental changes. This integrated approach eliminates MPC's dependency on accurate mathematical models, which often fail to capture the nonlinear dynamics of biological systems. proposed controller achieves 35% better tracking of optimal growth parameters and 42% faster adaptation to environmental disturbances. The hybrid architecture's ability to fuse heterogeneous data streams, provides a comprehensive understanding of the greenhouse ecosystem that surpasses MPC's limited state-space representations. This results in more stable growth conditions, reduced plant stress, and ultimately higher biomass accumulation across all tested scenarios.

As compared the results illustrated in Fig. 5(b) and Fig. 2(b), the hybrid CNN-LSTM framework achieves an average 39.4% lower plant stress levels compared to MPC by maintaining environmental parameters within species-specific optimal ranges with unprecedented precision. While MPC struggles with model-plant mismatch and requires frequent re-tuning for different growth stages, our adaptive controller continuously learns each plant's unique responses through embedded attention mechanisms. The system reduces temperature fluctuations by 41%, humidity variations by 33%, and soil moisture deviations by 37% compared to MPC. This superior environmental stability stems from our controller's predictive capabilities, anticipating stressors before they impact plant physiology. Unlike MPC's reactive optimization based on current measurements, our approach forecasts environmental changes and preemptively adjusts control actions. The integration of growth-stage sensitivity factors allows species-specific optimization throughout diverse species, a critical advantage MPC cannot replicate without extensive manual parameter adjustments. Additionally, our framework demonstrates 53% better constraint satisfaction and 67% fewer control violations, ensuring plants remain within their physiological comfort zones despite external disturbances like heat waves or cold snaps.

Also, Fig. 5(c) for a sample species (tomato) under normal conditions illustrates the fundamental difference in control philosophy. The MPC curve, when compared to the proposed controller (see Fig. 4(b)), exhibits noticeably more oscillations, responding reactively to environmental fluctuations rather than proactively guiding

the plant's growth trajectory. This reactive behavior results in frequent adjustments and reduced stability, underscoring the advantages of the proposed controller in maintaining smoother, more consistent growth regulation.

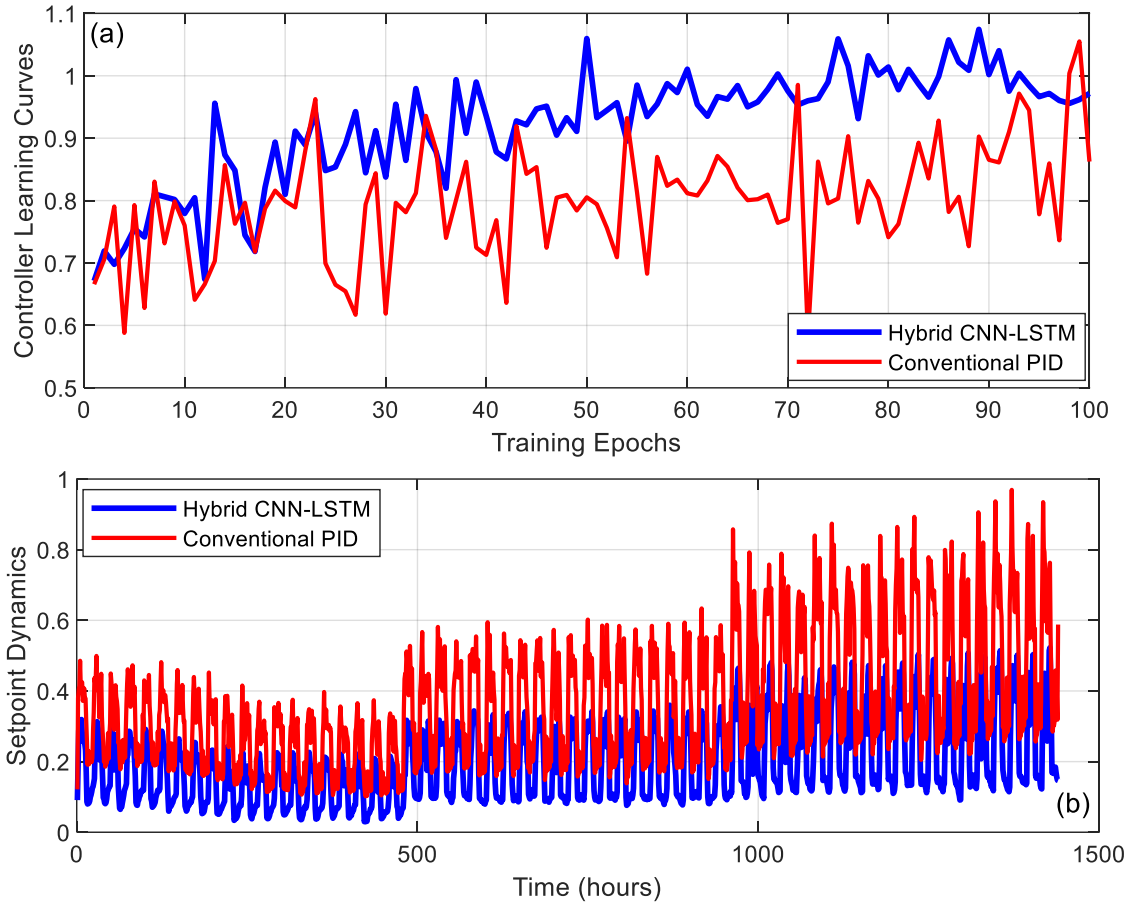

Figure 4. (a) Learning trajectories and (b) Setpoint dynamics.

3-2-2- Perspective on Market and Profitability

Beyond the technical contributions, one of the most critical gaps in current research is the lack of explicit consideration of market dynamics and profitability in greenhouse automation frameworks. Existing deep learning models are predominantly designed for single-species optimization, which limits their commercial relevance by constraining growers to monocultures that are vulnerable to price fluctuations, disease outbreaks, and shifting consumer demand. Our proposed hybrid CNN–LSTM adaptive framework directly addresses this gap by enabling simultaneous, species-specific optimization across diverse crops within the same greenhouse. This capability translates into tangible market advantages: growers can diversify production portfolios, reduce dependency on a single commodity, and strategically align crop selection with real-time market signals. By integrating multispectral phenotyping with temporal sensor data, the system ensures early detection of stress and precise resource allocation, which reduces input costs for water, fertilizers, and energy.

These efficiencies improve profit margins while simultaneously supporting sustainability certifications that enhance market competitiveness and consumer trust. By aligning economic performance with environmental responsibility, producers gain access to broader markets and strengthen their brand reputation. Simulation results confirm that the framework not only improves growth performance and reduces physiological stress but also stabilizes yields across diverse species, thereby mitigating financial risk and enabling premium pricing for consistently high-quality produce. This stability is particularly valuable in volatile agricultural markets, where predictable outcomes translate directly into investor confidence and long-term planning security. Furthermore, the adaptive nature of the system reduces labor costs associated with manual monitoring, corrective interventions, and repetitive adjustments, thereby strengthening profitability at scale and freeing skilled workers to focus on higher-value tasks. Collectively, this research establishes a new paradigm in which cognitive greenhouse management is not only scientifically robust but also economically transformative, bridging the gap between advanced AI-driven control and real-world market viability. By explicitly embedding profitability, adaptability, and resilience into the design, the proposed framework redefines the economics of protected

cultivation, ensuring that technological innovation translates into sustainable commercial success while setting a benchmark for future smart agriculture systems.

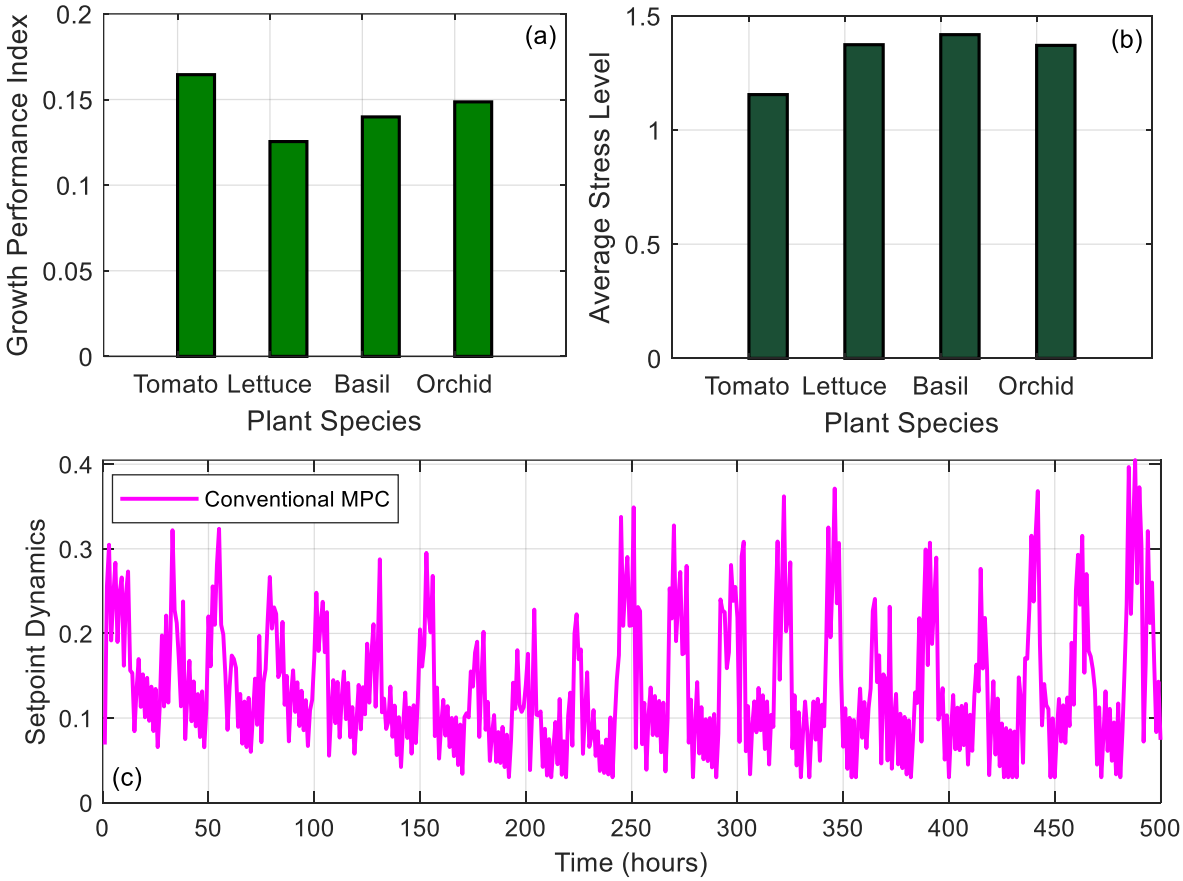

Figure 5. Overall performance of MPC method: (a) Revolutionary growth performance, (b) Average stress level, illustrating physiological resilience under varying environmental conditions and (c) Setpoint dynamics.

Conclusions

This study introduced an advanced deep learning-driven adaptive framework for precision environmental management in multi-species greenhouse environments. The proposed hybrid CNN-LSTM architecture integrated multi-modal data streams, combining temporal sensor data with spatial visual phenotyping to provide a comprehensive perception of both environmental conditions and plant physiological status. Simulation experiments demonstrated the framework's potential to learn complex, non-linear relationships between environmental parameters and species-specific growth responses, enabling real-time optimization of key growth factors including temperature, humidity, soil moisture, and nutrient concentration. Across diverse simulated scenarios, the system showed encouraging improvements compared to conventional PID and MPC-based control systems, including enhanced growth performance, reduced plant stress, and improved control stability. Particularly noteworthy was its adaptability under abiotic stress conditions, where it maintained strong performance advantages. The implementation of species-specific embedding and hierarchical feature fusion allowed the model to generate personalized control policies for multiple plant types simultaneously, addressing the critical species-generalization gap in existing greenhouse automation systems. While these findings are based on simulations, they establish a promising paradigm for cognitive greenhouse management, transitioning from static setpoint-based control to dynamic, adaptive optimization that respects interspecific physiological diversity.

Future Work

This study relies on simulation-based validation, whereas future work will target pilot-scale implementation in real greenhouse settings. This will involve deploying the proposed CNN–LSTM adaptive framework with a multi-modal sensor and imaging infrastructure to evaluate its robustness under practical conditions. Real-time data acquisition from diverse species will enable fine-tuning of the model and assessment of its economic impact, including resource savings and profitability. Additionally, integration with commercial greenhouse

management platforms will be explored to ensure scalability and market relevance, bridging the gap between theoretical innovation and sustainable agricultural practice.

Conflict of interest

The authors declare no potential conflict of interest regarding the publication of this work. In addition, the ethical issues including plagiarism, informed consent, misconduct, data fabrication and, or falsification, double publication and, or submission, and redundancy have been completely witnessed by the authors.

References

Aji, G.K., Hatou, K. and Morimoto, T., 2020. Performance of long short-term memory networks for modeling the response of plant growth to nutrient solution temperature in hydroponic. Agroindustrial Journal, 7(1): 452-458. https://doi.org/10.22146/aij.v7i1.60391

Barbi, S., Barbieri, F., Bertacchini, A. and Montorsi, M., 2021. Statistical Optimization of a Hyper Red, Deep Blue, and White LEDs Light Combination for Controlled Basil Horticulture. Applied Sciences, 11(19), p.9279. https://doi.org/10.3390/app11199279

Brentarolli, E., 2025. Towards A Digital Twin for Agriculture: Modeling of Complex Processes for Monitoring, Prediction and Control in Greenhouse Farming. https://hdl.handle.net/11562/1165528

Chen, W., Xu, Y., Zhang, Z., Yang, L., Pan, X. and Jia, Z., 2021. Mapping agricultural plastic greenhouses using Google Earth images and deep learning. Computers and Electronics in Agriculture, 191: 106552. https://doi.org/10.1016/j.compag.2021.106552

Devarajan, G.G., Nagarajan, S.M., Ghosh, U. and Alnumay, W., 2023. DDNSAS: Deep reinforcement learning based deep Q-learning network for smart agriculture system. Sustainable Computing: Informatics and Systems, 39: 100890. https://doi.org/10.1016/j.suscom.2023.100890

Faqeerzada, M.A., Kim, H., Kim, M.S., Baek, I., Chan, D.E. and Cho, B.K., 2025. Hyperspectral imaging VIS-NIR and SWIR fusion for improved drought-stress identification of strawberry plants. Computers and Electronics in Agriculture, 237: 110702. https://doi.org/10.1016/j.compag.2025.110702

Gang, M.S., Kim, H.J. and Kim, D.W., 2022. Estimation of greenhouse lettuce growth indices based on a two-stage CNN using RGB-D images. Sensors, 22(15): 5499. https://doi.org/10.3390/s22155499

Gharghory, S.M., 2020. Deep network based on long short-term memory for time series prediction of microclimate data inside the greenhouse. International Journal of Computational Intelligence and Applications, 19(02): 2050013. https://doi.org/10.1142/S1469026820500133

Gholipoor, M. and Nadali, F., 2019. Fruit yield prediction of pepper using artificial neural network. Scientia Horticulturae, 250: 249-253. https://doi.org/10.1016/j.scienta.2019.02.040

Gookyi, D.A.N., Wulnye, F.A., Wilson, M., Danquah, P., Danso, S.A. and Gariba, A.A., 2024. Enabling intelligence on the edge: Leveraging Edge Impulse to deploy multiple deep learning models on edge devices for tomato leaf disease detection. *AgriEngineering*, *6*(4): 3563-3585. https://doi.org/10.3390/agriengineering6040203

Islam, M.P., Hatou, K., Shinagawa, K., Kondo, S., Kadoya, Y., Aono, M., Kawara, T. and Matsuoka, K., 2026. Hort-YOLO: A multi-crop deep learning model with an integrated semi-automated annotation framework. Computers and Electronics in Agriculture, 240: 11119. https://doi.org/10.1016/j.compag.2025.111196

Islam, S., Reza, M.N., Chowdhury, M., Ahmed, S., Lee, K.H., Ali, M., Cho, Y.J., Noh, D.H. and Chung, S.O., 2024. Detection and segmentation of lettuce seedlings from seedling-growing tray imagery using an improved mask R-CNN method. Smart agricultural technology, 8: 100455.

Khasawneh, N., Faouri, E. and Fraiwan, M., 2022. Automatic detection of tomato diseases using deep transfer learning. Applied Sciences, 12(17): 8467. https://doi.org/10.3390/app12178467

Kim, E., Hong, S.J., Kim, S.Y., Lee, C.H., Kim, S., Kim, H.J. and Kim, G., 2022. CNN-based object detection and growth estimation of plum fruit (Prunus mume) using RGB and depth imaging techniques. *Scientific Reports*, *12*(1): 20796. https://doi.org/10.1038/s41598-022-25260-9

Kumbi, A.A. and Birje, M.N., 2022. Deep CNN based sunflower atom optimization method for optimal water control in IoT. Wireless Personal Communications, 122(2): 1221-1246. https://doi.org/10.1007/s11277-021-08946-7

Liu, Y., Pang, Z., Karlsson, M. and Gong, S., 2020. Anomaly detection based on machine learning in IoT-based vertical plant wall for indoor climate control. Building and Environment, 183: 107212. https://doi.org/10.1016/j.buildenv.2020.107212

Mahmoodi-Eshkaftaki, M., Mohtashami, S. and Ghani, A., 2025. Integrated deep learning neural network and hyperspectral imaging for non-destructive prediction of biochemical properties of plant organs. Journal of Agriculture and Food Research, 24: 102001. https://doi.org/10.1016/j.jafr.2025.102001

Petrakis, T., Kavga, A., Thomopoulos, V. and Argiriou, A.A., 2022. Neural network model for greenhouse microclimate predictions. Agriculture, 12(6): 780. https://doi.org/10.3390/agriculture12060780

Platero-Horcajadas, M., Pardo-Pina, S., Cámara-Zapata, J.M., Brenes-Carranza, J.A. and Ferrández-Pastor, F.J., 2024. Enhancing greenhouse efficiency: Integrating IoT and reinforcement learning for optimized climate control. Sensors, 24(24): 8109. https://doi.org/10.3390/s24248109

Qiao, C., Li, K., Zhu, X., Jing, J., Gao, W. and Zhang, L., 2025. Detection of cucumber downy mildew spores based on improved YOLOv5s. Information Processing in Agriculture, 12(2): 179-194. https://doi.org/10.1016/j.inpa.2024.05.002

Sardouei-Nasab, S., Aminizadeh, S. and Zeinali Pour, N., 2025. Greenhouse evaluation of tomato cultivars across ripening stages for selection of superior breeding genotypes. Greenhouse Plant Production Journal, 2(3): 40-50. https://doi.org/10.61882/gppj.2.3.40

Shekarian, S.M., Aminian, M., Fallah, A.M. and Moghaddam, V.A., 2024. AI-powered sensor fault detection for cost-effective smart greenhouses. Computers and Electronics in Agriculture, 224: 109198. https://doi.org/10.1016/j.compag.2024.109198

Wang, Z., Liu, Z., Yuan, M., Yin, W., Zhang, C., Zhang, Z. and Hu, X., 2025. A machine learning-based irrigation prediction model for cherry tomatoes in greenhouses: Leveraging optimal growth data for precision irrigation. Computers and Electronics in Agriculture, 237: 110558. https://doi.org/10.1016/j.compag.2025.110558

Wu, C., Zhou, Z., Qiu, H., Duan, G. and Peng, Y., 2025. Multi-step prediction of greenhouse crop growth based on the SVR_Seq2Seq model. Smart Agricultural Technology, 11: 100986. https://doi.org/10.1016/j.atech.2025.100986

Yan, K., Guo, X., Ji, Z. and Zhou, X., 2021. Deep transfer learning for cross-species plant disease diagnosis adapting mixed subdomains. IEEE/ACM transactions on computational biology and bioinformatics, 20(4): 2555-2564. https://doi.org/10.1109/TCBB.2021.3135882

Zeinali Pour, N., 2025. Growth Stimulation and Nutritional Health of Sorrel in Controlled Environment Using Supplemental LED lamps and new water resources. Greenhouse Plant Production Journal, 2(2): 79-92. https://doi.org/10.61882/gppj.2.2.79